MEDICAL SCIENCE MONITOR

CLINICAL RESEARCH

e-ISSN 1643-3750
© Med Sci Monit, 2017; 23: 1552-1558
DOI: 10.12659/MSM.899966

Received: 2016.06.07
Accepted: 2016.07.11
Published: 2017.03.31

Diagnostic Value of Semiquantitative Analysis of ^{99m}Technetium-Methoxyisobutylisonitrile (^{99m}Tc-MIBI Imaging in Predicting Early-Stage Cervical Lymph Node Metastasis of Thyroid Carcinoma

Authors' Contribution:
Study Design A
Data Collection B
Statistical Analysis C
Data Interpretation D
Manuscript Preparation E
Literature Search F
Funds Collection G

BC 1 Xiao-Chun Zhu
BC 2 Kai Zhou
CE 1 Shi-Qing Xu
AB 1 Yu-Bo Ma

1 Department of Nuclear Medicine, Shanghai 9th People's Hospital, Shanghai JiaoTong University School of Medicine, Shanghai, P.R. China
2 Department of Laboratory, Shanghai 9th People's Hospital, Shanghai JiaoTong University School of Medicine, Shanghai, P.R. China

Corresponding Authors: Yu-Bo Ma, e-mail: myb7802@126.com & Xiao-Chun Zhu, e-mail: nashdirky@163.com
Source of support: Departmental sources

Background: The aim of this study was to evaluate the value of semiquantitative analysis (SQA) of ^{99m}Tc-MIBI imaging in predicting early-stage cervical lymph node metastasis (CLNM) in thyroid carcinoma (TC).

Material/Methods: TC patients (n=106) undergoing surgical resection and histopathological examination were enrolled. All patients received ^{99m}Tc-MIBI imaging prior to surgery. P-glycoprotein (P-gp) expression was detected by PT-PCR and immunohistochemistry. With pathological results as the criterion standard, the diagnostic efficiency of ^{99m}Tc-MIBI imaging in predicting early-stage CLNM was evaluated. The correlation of P-gp with ^{99m}Tc-MIBI imaging was investigated. Logistic regression analysis was applied for analyzing the factors affecting early-stage CLNM.

Results: The detection rate and misdiagnosis rate of ^{99m}Tc-MIBI imaging for early-stage CLNM diagnosis were 87.3% and 12.7%, respectively. Receiver operating characteristic (ROC) curve analysis showed an accuracy of ^{99m}Tc-MIBI imaging of 85.85%. Preoperative ^{99m}Tc-MIBI scan showed statistical differences between metastasis and non-metastasis groups in early and delayed T/NT and washout rate (all $P<0.05$). The percentage of P-gp-expressing cells and the expression rate of *P-gp* gene both exhibited statistical differences between metastasis and no-metastasis groups (both $P<0.05$). Tumor diameter, lesion distribution, the percentage of P-gp-expressing cells, and the expression rate of *P-gp* gene were risk factors for CLNM (all $P<0.05$).

Conclusions: ^{99m}Tc-MIBI imaging has value in qualitative diagnosis of early-stage CLNM in TC. Tumor diameter, lesion distribution, the percentage of P-gp-expressing cells, and the expression rate of *P-gp* gene were risk factors for CLNM.

MeSH Keywords: Diagnosis • P-Glycoprotein • Thyroid Neoplasms

Full-text PDF: http://www.medscimonit.com/abstract/index/idArt/899966

2177 4 4 22

Indexed in: [Current Contents/Clinical Medicine] [SCI Expanded] [ISI Alerting System] [ISI Journals Master List] [Index Medicus/MEDLINE] [EMBASE/Excerpta Medica] [Chemical Abstracts/CAS] [Index Copernicus]

Background

Thyroid carcinoma (TC) is the most common endocrine malignancy, accounting for approximately 1% of all types of human cancer, with an increasing incidence reported worldwide [1]. Over 95% of TC derives from follicular epithelial cells, consisting of well-differentiated carcinoma (90~95% of TC) and poorly-differentiated and anaplastic carcinomas (1~2% of TC), whereas 3~5% of TC is a malignancy of parafollicular C cells derived from the neural crest [2]. It was reported that the incidence of cervical lymph node metastasis (CLNM) in patients with well-differentiated TC reached up to 20~90%, and that the metastatic spread of TC to cervical lymph nodes increases the risk of local or regional recurrence of the tumor and the need for further surgery [3]. Currently, preoperative ultrasonography is considered to be the most valuable option in predicting CLNM, but the sensitivity of ultrasound in detecting CLNM is not very high [4]. In recent years, novel imaging techniques for diagnosing malignant tumors has increasingly emerged, providing new insights into the early diagnosis of thyroid lesions [5,6].

^{99m}Technetium-methoxyisobutylisonitrile (^{99m}Tc-MIBI) is a non-specific tumor-philic imaging agent, commonly used in nuclear medicine due to its various advantages, including good physical and chemical characteristics, low cost, and easy-to-use properties [5]. Initially, ^{99m}Tc-MIBI was applied in myocardial perfusion scintigraphy, and has been widely used for diagnosing many malignancies, such as TC, breast cancer, lung cancer, and bone cancer [7]. On the other hand, P-glycoprotein (P-gp), belonging to the ATP-binding cassette (ABC) family of transport proteins, is a transmembrane protein encoded by *multidrug resistance 1* (*MDR1*) and expressed in tumor cells as well as some healthy tissues, whose overexpression results in lower levels of intracellular anticancer drug due to its drug efflux function, and thus has been linked to resistant cancers [8,9]. In addition, P-gp is also involved in regulation of apoptosis and proliferation, as well as invasion of malignant cells, showing prognostic value in several neoplasms [10,11]. Therefore, we hypothesized that P-gp may also be involved in the pathology and prognosis of TC. The present study explored the relationship between P-gp expression level and ^{99m}Tc-MIBI imaging and evaluated the value of semiquantitative analysis (SQA) of ^{99m}Tc-MIBI imaging for diagnosis of early-stage CLNM in TC patients, so as to increase the probability of early diagnosis and treatment of TC.

Material and Methods

Ethical statement

The study was approved by the Ethics Committee of Shanghai Ninth People's Hospital, Shanghai JiaoTong University School of Medicine and written informed consent was obtained from each eligible participant.

Subjects

A total of 106 patients diagnosed with TC (25 men and 81 women; aged 46.9±13.1 years) in Shanghai Ninth People's Hospital between February 2014 and August 2015 were enrolled. The exclusion criteria were: (1) patients who underwent cervical lymphadenectomy or neck dissection; (2) incomplete clinical or pathological data; (3) thyroid cancer recurrence; and (4) malignant tumors with distant metastasis to thyroid glands. All patients underwent operations, with 106 TC specimens and 106 cases of corresponding para-carcinoma tissues analyzed by histopathology.

SQA of ^{99m}Tc-MIBI imaging

Patients were intravenously injected with 740 MBq ^{99m}Tc-MIBI before dual-phase ^{99m}Tc-MIBI scintigraphy of parts of thyroid glands (the anterior aspect) was performed, using a conventional low-energy parallel-hole collimator with an energy peak of 140 keV and a window width of 20%. The magnification when performing scanning was 2.19-fold, with a matrix of 256×256 pixels. The early and delayed images were obtained 10 mins before radiotracer injection and 120 mins after radiotracer injection (1 frame for the early phase or the delayed phase; 5 mins for each frame). Scintigraphy results were compared with type-B ultrasonic results by 3 experienced nuclear medicine physicians, who chose a region of interest (ROI) of the same size from the early image or the delayed image, according to the thyroid lesions implicated by the 2 above-mentioned imaging methods. The radioactive counts in a ROI and the counterpart (representing normal thyroid tissues) of the same image are expressed by T and NT, correspondingly. The radioactive count ratios (T/NT) of the early phase and the delayed phase were then calculated. T/NT >1.08 showed positive results. After attenuation correction, the ^{99m}Tc-MIBI washout rate was calculated, following the equation: washout rate=$T_{\text{early phase}}-T_{\text{delayed phase}}/T_{\text{early phase}}\times 100\%$.

Immunohistochemistry (IHC)

According to the IHC kit protocol (ZSGB Bio-Technique Co., Ltd., Beijing, China), ICH staining for P-glycoprotein (P-gp) was performed by the streptavidin-peroxidase (SP) method. Positive expression of P-gp was located in cell membrane or cytoplasm, shown as brown-yellow granules. For each slide, 5 microscopic fields under high-power magnification were chosen, and 200 cells in every field were counted for the calculation of the percentage of positive cells per 1000 cells. A percentage less than 10% was defined as negative expression.

Indexed in: [Current Contents/Clinical Medicine] [SCI Expanded] [ISI Alerting System] [ISI Journals Master List] [Index Medicus/MEDLINE] [EMBASE/Excerpta Medica] [Chemical Abstracts/CAS] [Index Copernicus]

Table 1. RT-qPCR primer sequence.

Gene	Primer sequence
P-gp	Sense primer: 5'-gcaagtcngttcatttgctc-3'
	Antisense primer: 5'-cacaatctcttcclgtgacac-3'
β-actin	Sense primer: 5'-gaeaacgget ccggcatgtg-3'
	Antisense primer: 5'-gaccttcaacaccccagcca-3'

RT-qPCR – real-time quantitative fluorescence polymerase chain reaction.

Real-time quantitative fluorescence polymerase chain reaction (RT-qPCR)

Following the instructions of the mRNA Purification Minikit (Qiagen, Germany), mRNA was separated from total RNA extracted from TC specimens and its para-carcinoma tissues. Databases of the National Center for Biotechnology Information (NCBI) were searched for complete sequences of *P-gp*, *β-actin*, and the corresponding mRNAs. Primers (Table 1) were designed with Primer Premier 5.0 software, and further optimized for better specificity based on the comparisons of primer sequences using BLAST software in the NCBI databases. The volume of the PCR system was 25 μL and the PCR kit was purchased from Invitrogen (USA). The staining results were read under an ultraviolet (UV) transilluminator and we used Quantity One software for gray-scale value analyses. Positive results were shown as 2 strips representing the internal reference (372 bp) and *P-gp* (480 bp), respectively. The ratio of integral absorbance (Ai) values of 2 strips was associated with the relative expression of *P-gp*. $Ai_{(P\text{-}gp)}/Ai_{(internal\ reference)}$ <0.1 showed negative results.

Statistical analysis

SPSS 21.0 software (SPSS Inc., Chicago, IL, USA) was used for statistical analysis. The measurement data were expressed as mean ± standard deviation ($\bar{\chi}\pm$SD) and analyzed by *t* test. The enumeration data are expressed in percentage and assessed using the chi-square test. A receiver operating characteristic (ROC) curve was employed to illustrate the performance of SQA of ^{99m}Tc-MIBI imaging for diagnosis of early-stage CLNM in TC. Pearson product-moment correlation coefficient was used for correlation analyses. Logistic regression analysis was applied for analyses of factors related to CLNM. $P<0.05$ showed a statistically significant difference.

Results

Clinical data

The pathological results of the operations from 106 TC patients showed 71 patients with CLNM and 35 without CLNM. Based on the pathological results, the TC patients were assigned into 2 groups: the metastasis group and the non-metastasis group.

Table 2. Comparisons of clinical data between the metastasis group and the non-metastasis group.

	Metastasis group (n=71)	Non-metastasis group (n=35)	*P*
Age			0.012
<45 years	52	17	
≥45 years	19	18	
Gender			0.038
Male	21	4	
Female	50	31	
Tumor diameter			< 0.001
≤1 cm	6	18	
>1 cm	65	17	
Lesion distribution			0.001
Unilateral	46	33	
Bilateral	25	2	
Combined occurrence of HT			0.095
Yes	19	15	
No	52	20	

HT – Hashimoto's thyroiditis.

Indexed in: [Current Contents/Clinical Medicine] [SCI Expanded] [ISI Alerting System] [ISI Journals Master List] [Index Medicus/MEDLINE] [EMBASE/Excerpta Medica] [Chemical Abstracts/CAS] [Index Copernicus]

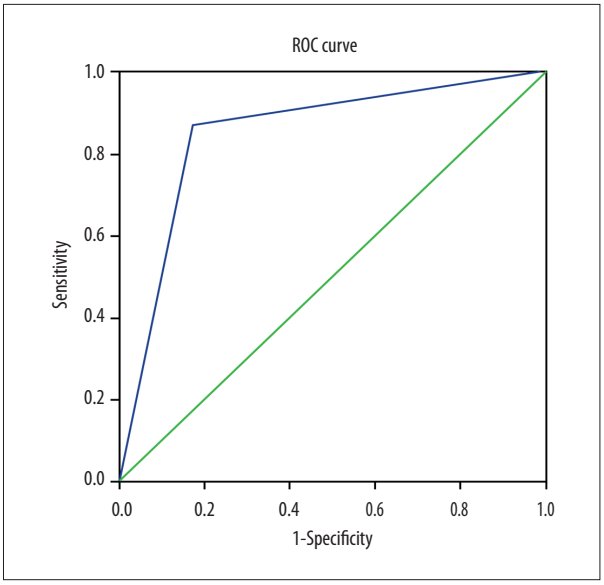

Figure 1. ROC curve analysis showing the performance of SQA of 99mTc-MIBI imaging for diagnosis of early-stage CLNM in TC patients. ROC – receiver operating characteristic; SQA – semiquantitative analysis; CLNM – cervical lymph node metastasis; TC – thyroid carcinoma.

There were statistically significant differences between the 2 groups in multiple items, including age (<45 years/≥45 years), sex (male/female), tumor diameter (≤1 cm/>1 cm), and lesion distribution (unilateral/bilateral) (all $P<0.05$), except for the combined occurrence of Hashimoto's thyroiditis (HT) (yes/no) ($P>0.05$) (Table 2).

Performance of SQA of 99mTc-MIBI imaging for diagnosis of early-stage CLNM in TC

The results of 99mTc-MIBI imaging showed 68 TC patients with CLNM and 38 without CLNM; among them, there were 6 false-positives and 9 false-negatives. Using the pathological results as reference, the detection rate and the misdiagnosis rate of 99mTc-MIBI imaging for diagnosis of early-stage CLNM was 87.3% and 12.7%, respectively, and the false-positive rate and false-negative rates were 8.45% and 25.7%, respectively. The ROC curve analysis of the results of 99mTc-MIBI imaging (Figure 1) showed that the area under the ROC curve was 0.851, and the sensitivity, specificity, and accuracy of 99mTc-MIBI imaging in diagnosing CLNM were 87.3%, 82.86%, and 85.85%, respectively ($P<0.05$).

Relationship of SQA parameters and CLNM

The SQA parameters of 99mTc-MIBI imaging included T/NT of the early phase and the delayed phase, as well as the washout rate. Before operations, there were significant differences between the metastasis group and the non-metastasis group in terms of all the above-mentioned SQA parameters of 99mTc-MIBI imaging (all $P<0.05$) (Table 3).

Expression level of P-gp

As seen in Figure 2, immunohistochemical results demonstrated that the positive expression of P-gp was mainly located in cell membranes (yellow-brown granules) but seldom in cytoplasm. The percentage of P-gp-expressing cells exhibited a significant difference between the metastasis group (41.0±8.36%) and the non-metastasis group (27.0±7.02%) ($P<0.05$). In the metastasis group and the non-metastasis groups, the expression rates of *P-gp* gene were 0.64±0.13 and 0.33±0.18, respectively, showing a statistically significant difference ($P<0.05$) (Figure 3).

Relationship of P-gp levels with 99mTc-MIBI imaging

The correlation analyses of the percentages of P-gp-expressing cells and the washout rates of 99mTc-MIBI imaging in 106 cases of TC specimens demonstrated a remarkably positive correlation ($r=0.621$, $P<0.001$). According to the correlation analyses in 106 TC specimens, there was a linear positive relationship between the expression rates of *P-gp* and the washout rates of 99mTc-MIBI imaging ($r=0.580$, $P<0.001$) (Figure 4).

Logistic regression analysis

With CLNM as an independent variable and statistically significant factors (age, sex, tumor diameter, lesion distribution, the percentage of P-gp-expressing cells, and the expression rate of *P-gp* gene) from clinical data as dependent variables, logistic regression analyses were carried out. The results indicated that tumor diameter, lesion distribution, the percentage of P-gp-expressing cells, and the expression rate of *P-gp* gene were risk factors to CLNM (all OR >1, $P<0.001$) (Table 4).

Table 3. Relationship of SQA parameters with CLNM.

	Metastasis group	Non-metastasis group	*P*
T/NT of the early phase	1.21±0.26	1.55±0.24	<0.001
T/NT of the delayed phase	1.19±0.25	1.66±0.28	<0.001
Washout rate (%)	17.20±2.94	7.10±3.23	<0.001

SQA – semiquantitative analysis; CLNM – cervical lymph node metastasis; T/NT – radioactive count ratios.

Indexed in: [Current Contents/Clinical Medicine] [SCI Expanded] [ISI Alerting System] [ISI Journals Master List] [Index Medicus/MEDLINE] [EMBASE/Excerpta Medica] [Chemical Abstracts/CAS] [Index Copernicus]

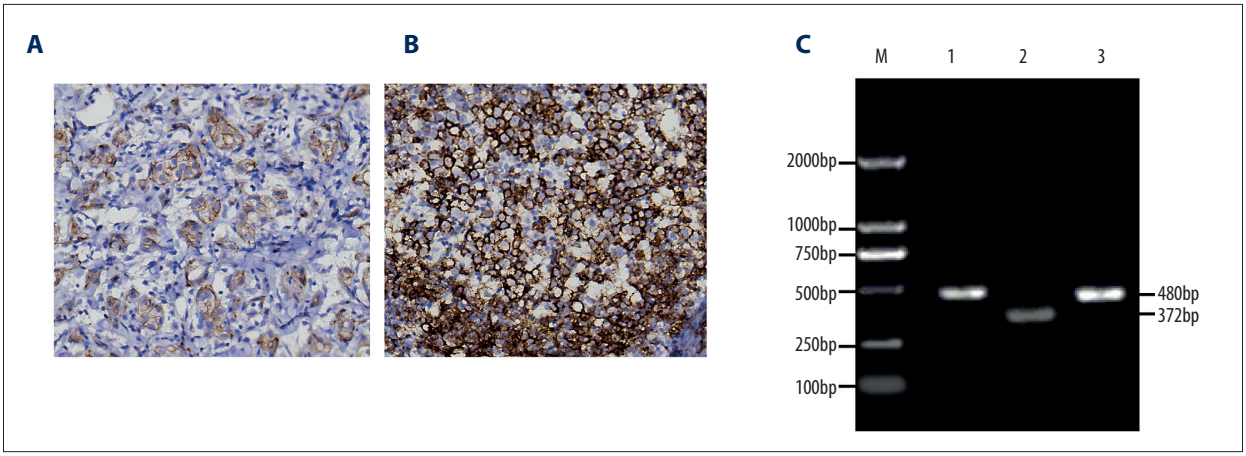

Figure 2. The IHC results of P-pg and the PCR results of *P-pg* in TC specimens and para-carcinoma tissues. (**A**) The IHC results of P-pg in TC specimens. (**B**) The IHC results of P-pg in para-carcinoma tissues. (**C**) The PCR results of *P-pg* in TC specimens and its para-carcinoma tissues: 1 – the PCR result of *P-pg* in para-carcinoma tissues; 2 – the PCR result of the internal reference; 3 – the PCR result of *P-pg* in TC specimens. TC – thyroid carcinoma.

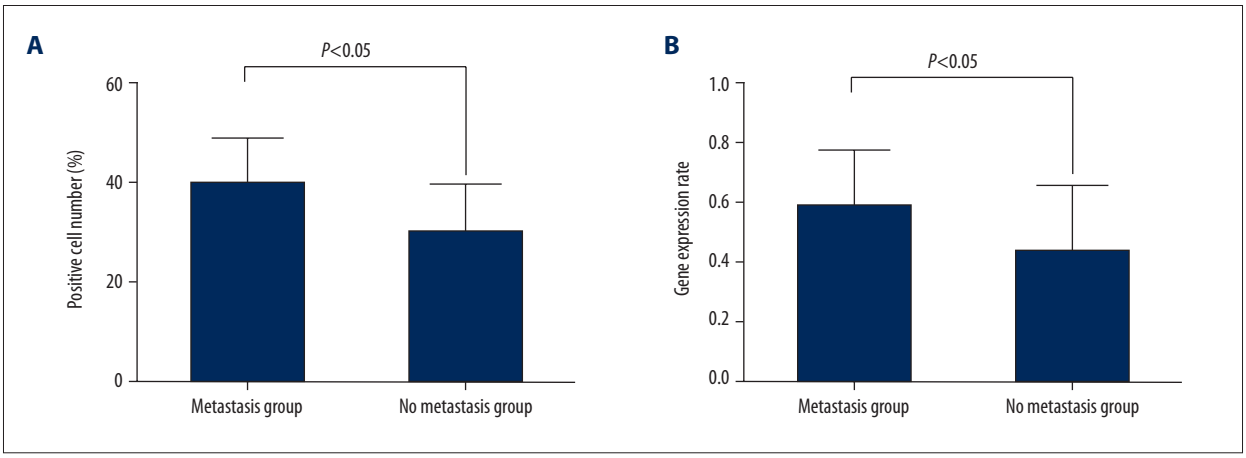

Figure 3. Comparisons of the percentage of P-gp-expressing cells (**A**) and the expression rate of *P-gp* gene (**B**) between the metastasis group and the non-metastasis group.

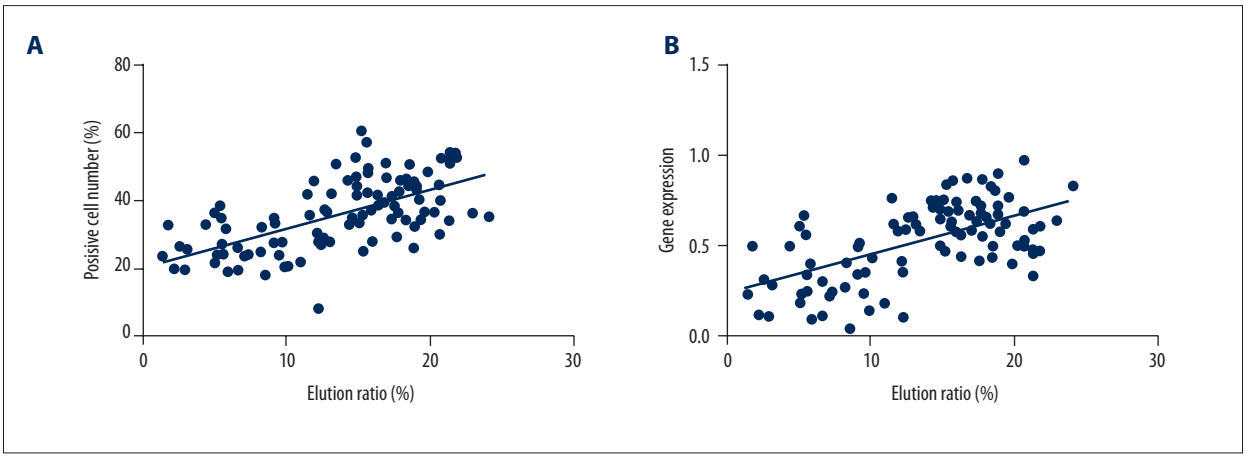

Figure 4. Relationship of P-gp levels and ^{99m}Tc-MIBI imaging. (**A**) Relationship of the percentage of P-gp-expressing cells with the washout rate of ^{99m}Tc-MIBI imaging. (**B**) Relationship of the expression rate of *P-gp* gene with the washout rate of ^{99m}Tc-MIBI imaging.

Indexed in: [Current Contents/Clinical Medicine] [SCI Expanded] [ISI Alerting System] [ISI Journals Master List] [Index Medicus/MEDLINE] [EMBASE/Excerpta Medica] [Chemical Abstracts/CAS] [Index Copernicus]

Table 4. Logistic regression analyses of the metastasis group and the non-metastasis group.

	β	S.E.	Wald	Sig.	OR	95% C.I.	
						Lower	Upper
Gender	–1.484	0.847	3.069	0.080	0.227	0.043	1.193
Tumor diameter	1.961	0.746	6.922	0.009	7.109	1.649	30.649
Lesion distribution	2.680	0.944	8.061	0.005	14.585	2.293	92.772
Age	0.253	0.702	0.130	0.719	1.288	0.325	5.100
The percentage of P-gp-expressing cells	0.095	0.035	7.371	0.007	1.100	1.027	1.179
The expression rate of *P-gp* gene	4.289	1.525	7.909	0.005	72.879	3.668	1447.840

β – partial regression coefficient; S.E. – standard error; Sig. – significance; OR – odds ratio; C.I. – confidence interval.

Discussion

TC is the most common endocrine malignancy, accompanied by metastasis in local cervical lymph nodes [12]. Thus, it is necessary to search for effective methods in diagnosing CLNM, which to some extent plays a positive role in the treatment of TC.

The present study found that ^{99m}Tc-MIBI imaging can be used to detect early-stage CLNM and corresponding SQA parameters, as well as to predict the possibilities of CLNM. ^{99m}Tc-MIBI is a lipophilic cationic complex that enters cells by active transportation to the cell membrane, which has been widely used in nuclear medicine for the diagnostic imaging of the myocardium and parathyroid [13]. Since ^{99m}Tc-MIBI retention is correlated with the number and activity of mitochondria, ^{99m}Tc-MIBI is absorbed quickly and accumulated in mitochondria-rich tumor cells [14]. Moreover, based on the fact that tumor cell metabolism is characterized by fast absorption and slow elimination, tumor cells were easily distinguished from normal issues under the effect of a nonspecific tumor-philic imaging agent ^{99m}Tc-MIBI [5]. In addition, dual-phase ^{99m}Tc-MIBI scintigraphy showed either a relatively progressive increase over time or a fixed uptake that persisted on the delayed imaging in cancer lesions, contrary to the uptake in the surrounding thyroid tissues [15], and thus could be applied to exclude many benign lesions, such as inflammation. It was reported that in TC patients with metastases without ^{131}I uptake, ^{99m}Tc-MIBI scan was very useful in diagnosing local recurrence and/or mediastinal metastases [16]. Thus, as a non-invasive and reliable diagnostic tool, ^{99m}Tc-MIBI scintigraphy plays an important role in monitoring TC and other malignancies [17].

However, it had also been demonstrated that both the percentage of P-gp-expressing cells and the expression rate of *P-gp* gene were much higher in the metastasis group than in the non-metastasis group, and that both the percentage of P-gp-expressing cells and the expression rate of *P-gp* gene were positively correlated with the washout rate of ^{99m}Tc-MIBI imaging. P-gp is an active efflux pump that extrudes a large variety of chemotherapeutic drugs from the cells, leading to insufficient accumulation of drugs in the target tissues [18]. It has been confirmed that ^{99m}Tc-MIBI, a lipophilic cationic complex, is a suitable transport substrate for P-gp and is widely used for tumor imaging [19]. Since ^{99m}Tc-MIBI is able to accumulate in tumor cells and is then excreted by P-gp, a tumor with only faint uptake of ^{99m}Tc-MIBI likely has high P-gp expression [20]. Therefore, considering the higher expression of P-gp in the metastasis group than the non-metastasis group and the biological function of ^{99m}Tc-MIBI and P-gp, it was further confirmed that ^{99m}Tc-MIBI imaging could be used for the qualitative diagnosis of early-stage CLNM in TC. Also, it is reasonable to speculate that the P-gp expression exhibits a positive correlation with the washout rate of ^{99m}Tc-MIBI. In addition, a case report of a patient with malignant schwannoma after chemotherapy showed that the P-gp expression was much higher in the metastatic lesion than in the primary lesion [21], which was consistent with our results in TC. Although P-gp is a membrane efflux pump that has a role in the excretion of ^{99m}Tc-MIBI in tumors, P-gp expression has been confirmed to be not correlated with ^{99m}Tc-MIBI uptake in tumors [22]. Thus, P-gp, only functioning to increase the drug clearance from the cells, was not a confounding factor for ^{99m}Tc-MIBI imaging in the detection of CLNM in TC.

Conclusions

In conclusion, our study suggests that SQA parameters of ^{99m}Tc-MIBI imaging could be applied to detect early-stage CLNM in TC patients. Moreover, the ^{99m}Tc-MIBI washout rate was positively correlated with the P-gp expression. We found that tumor diameter, lesion distribution, the percentage of P-gp-expressing cells, and the expression rate of *P-gp* gene were factors affecting the occurrence of CLNM. However, the results of this study are limited due to its small sample size. Further studies are needed to validate the clinical value of SQA parameters of ^{99m}Tc-MIBI imaging in diagnosing early-stage CLNM of TC.

Indexed in: [Current Contents/Clinical Medicine] [SCI Expanded] [ISI Alerting System] [ISI Journals Master List] [Index Medicus/MEDLINE] [EMBASE/Excerpta Medica] [Chemical Abstracts/CAS] [Index Copernicus]

Acknowledgments

We would like to acknowledge the helpful comments on this paper received from our reviewers.

Competing interests

None.

References:

1. Shirazi HA, Hedayati M, Daneshpour MS et al: Analysis of loss of heterozygsity effect on thyroid tumor with oxyphilia cell locus in familial non medullary thyroid carcinoma in Iranian families. Indian J Hum Genet, 2012; 18(3): 340–43
2. Ria R, Simeon V, Melaccio A et al: Gene expression profiling of normal thyroid tissue from patients with thyroid carcinoma. Oncotarget, 2016; 7(20): 29677–88
3. Jung JH, Kim CY, Son Sh et al: Preoperative prediction of cervical lymph node metastasis using primary tumor SUVmax on 18F-FDG PET/CT in patients with papillary thyroid carcinoma. PLoS One, 2015; 10(12): e0144152
4. Wang QC, Cheng W, Wen X et al: Shorter distance between the nodule and capsule has greater risk of cervical lymph node metastasis in papillary thyroid carcinoma. Asian Pac J Cancer Prev, 2014; 15(2): 855–60
5. Pan X, Duan D, Zhu Y et al: Values of (99m)Tc-methoxyisobutylisonitrile imaging after first-time large-dose (131)I therapy in treating differentiated thyroid cancer. Onco Targets Ther, 2016; 9: 723–30
6. Saggiorato E, Angusti T, Rosas R et al: 99mTc-MIBI Imaging in the presurgical characterization of thyroid follicular neoplasms: Relationship to multidrug resistance protein expression. J Nucl Med, 2009; 50(11): 1785–93
7. Karacavus S, Ede H, Sarikaya S et al: The importance of the incidental thyroid gland uptake during Tc-99m MIBI myocardial perfusion scintigraphy. Eur Rev Med Pharmacol Sci, 2015; 19(15): 2781–85
8. Chen CY, Liu NY, Lin HC et al: Synthesis and bioevaluation of novel benzodipyranone derivatives as P-glycoprotein inhibitors for multidrug resistance reversal agents. Eur J Med Chem, 2016; 118: 219–29
9. Bessadok A, Garcia E, Jacquet H et al: Recognition of sulfonylurea receptor (ABCC8/9) ligands by the multidrug resistance transporter P-glycoprotein (ABCB1): Functional similarities based on common structural features between two multispecific ABC proteins. J Biol Chem, 2011; 286(5): 3552–69
10. Li DW, Gao S, Shen B et al: Effect of apoptotic and proliferative indices, P-glycoprotein and survivin expression on prognosis in laryngeal squamous cell carcinoma. Med Oncol, 2011; 28(Suppl. 1): S333–40
11. Kim JW, Park Y, Roh JL et al: Prognostic value of glucosylceramide synthase and P-glycoprotein expression in oral cavity cancer. Int J Clin Oncol, 2016 [Epub ahead of print]
12. Xu D, Wang L, Long B et al: Radiofrequency ablation for postsurgical thyroid removal of differentiated thyroid carcinoma. Am J Transl Res, 2016; 8(4): 1876–85
13. Maucksch U, Runge R, Wunderlich G et al: Comparison of the radiotoxicity of the Tc-labeled compounds Tc-pertechnetate, Tc-HMPAO and Tc-MIBI. Int J Radiat Biol, 2016 [Epub ahead of print]
14. Benard F, Lefebvre B, Beuvon F et al: Rapid washout of technetium-99m-MIBI from a large parathyroid adenoma. J Nucl Med, 1995; 36(2): 241–43
15. Chang MC, Tsai SC, Lin WY: Dual-phase 99mTc-MIBI parathyroid imaging reveals synchronous parathyroid adenoma and papillary thyroid carcinoma: A case report. Kaohsiung J Med Sci, 2008; 24(10): 542–47
16. Ronga G, Ventroni G, Montesano T et al: Sensitivity of [99mTc]methoxyisobutylisonitrile scan in patients with metastatic differentiated thyroid cancer. Q J Nucl Med Mol Imaging, 2007; 51(4): 364–71
17. Nikoletic K, Lucic S, Peter A et al: Lung 99mTc-MIBI scintigraphy: Impact on diagnosis of solitary pulmonary nodule. Bosn J Basic Med Sci, 2011; 11(3): 174–79
18. Krasznai ZT, Toth A, Mikecz P et al: Pgp inhibition by UIC2 antibody can be followed *in vitro* by using tumor-diagnostic radiotracers, 99mTc-MIBI and 18FDG. Eur J Pharm Sci, 2010; 41(5): 665–69
19. Chai X, Liu Q, Shao W et al: Bromocriptine enhances the uptake of (99m)Tc-MIBI in patients with hepatocellular carcinoma. J Biomed Res, 2012; 26(3): 165–69
20. Si H, Li X: Abundant blood supply and low P-glycoprotein expression on dynamic 99mTc-MIBI imaging predicted better chemotherapy sensitivity for a breast cancer patient: A case report. J Nucl Med Technol, 2012; 40(2): 89–91
21. Suto R, Abe Y, Lee YH et al: A case of malignant schwannoma with overexpression of multidrug resistance gene (MDR1) after chemotherapy. Anticancer Res, 1997; 17(3C): 2273–77
22. Jorna FH, Hollema H, Hendrikse HN et al: P-gp and MRP1 expression in parathyroid tumors related to histology, weight and (99m)Tc-sestamibi imaging results. Exp Clin Endocrinol Diabetes, 2009; 117(8): 406–12

Indexed in: [Current Contents/Clinical Medicine] [SCI Expanded] [ISI Alerting System] [ISI Journals Master List] [Index Medicus/MEDLINE] [EMBASE/Excerpta Medica] [Chemical Abstracts/CAS] [Index Copernicus]